

# SUPERFLUID TURBULENCE AND PULSAR GLITCH STATISTICS

A. MELATOS<sup>1</sup> AND C. PERALTA<sup>1,2</sup>  
 a.melatos@physics.unimelb.edu.au  
 Draft version November 2, 2018

## ABSTRACT

Experimental evidence is reviewed for the existence of superfluid turbulence in a differentially rotating, spherical shell at high Reynolds numbers ( $Re \gtrsim 10^3$ ), such as the outer core of a neutron star. It is shown that torque variability increases with  $Re$ , suggesting that glitch activity in radio pulsars may be a function of  $Re$  as well. The  $Re$  distribution of the 67 glitching radio pulsars with characteristic ages  $\tau_c \leq 10^6$  yr is constructed from radio timing data and cooling curves and compared with the  $Re$  distribution of all 348 known pulsars with  $\tau_c \leq 10^6$  yr. The two distributions are different, with a Kolmogorov-Smirnov probability  $\geq 1 - 3.9 \times 10^{-3}$ . The conclusion holds for (modified) Urca and nonstandard cooling, and for Newtonian and superfluid viscosities.

*Subject headings:* dense matter — hydrodynamics — stars: interior — stars: neutron — stars: rotation

## 1. INTRODUCTION

The known number of glitching radio pulsars has quadrupled in the last four years, as has the total number of glitches, in the wake of the Parkes Multibeam Survey and improved multifrequency timing solutions (Peralta 2006). Out of a total population of 1730 pulsars, 101 have experienced a total of 287 glitches (Wang et al. 2000; Krawczyk et al. 2003; Hobbs et al. 2004; Janssen & Stappers 2006). The enlarged data set invites an updated statistical study. Previous analyses identified certain empirical trends, e.g., glitch activity and healing parameter versus characteristic age (Shemar & Lyne 1996; Urama & Okeke 1999; Wang et al. 2000), and glitch amplitude versus recurrence time (Middleditch et al. 2006), while refuting certain theoretically predicted correlations, e.g., glitch amplitude versus spin period  $P$ , period derivative  $\dot{P}$ , and total spin down since the last glitch (“reservoir model”) (Shemar & Lyne 1996; Wang et al. 2000).

On the theoretical front, the global pattern of superfluid circulation in the outer core of a neutron star was recently computed numerically for the first time (Peralta et al. 2005, 2006a,b). In general, a fluid contained in a differentially rotating, spherical shell flows unsteadily under a wide range of conditions, especially in thick shells and at high Reynolds numbers  $Re \gtrsim 10^3$  (Junk & Egbers 2000). Such unsteady flow is observed in numerical and laboratory experiments with viscous fluids, e.g., transitions between Taylor vortex states (Marcus & Tuckerman 1987), Taylor vortex oscillations (Hollerbach 1998), relaminarization (Nakabayashi et al. 2005), and nonaxisymmetric modes on the route to high- $Re$  turbulence, like Taylor-Görtler vortices (Li 2004). Time-dependent flow is also observed in superfluids like helium II, e.g., torque “steps” and quasiperiodic torque oscillations in Couette and spin-up experiments (Tsakadze & Tsakadze 1980).

In this Letter, we combine theory and observation to test whether superfluid turbulence exists in neutron stars, as originally proposed by Greenstein (1970). In §2, we

present numerical simulations of a  $^1\text{S}_0$ -paired neutron superfluid in the outer core of a neutron star as the crust spins down electromagnetically. We show that the torque is steady for  $Re \lesssim 10^3$  and unsteady (e.g., oscillatory) otherwise. In §3, we combine standard cooling curves with measurements of the characteristic ages of radio pulsars to compute the temperature, viscosity, and hence  $Re$  of the star. We show that the  $Re$  distributions of those pulsars that glitch, and those that do not, are different — a rare instance of regularity in the glitch phenomenon. The implications for the existence of superfluid turbulence in neutron stars are weighed critically in §4.

## 2. HYDRODYNAMIC SUPERFLUID TURBULENCE

Large-scale, time-dependent, meridional circulation, driven by Ekman pumping, is a generic feature of viscous and superfluid flow in spherical Couette geometry (i.e., a differentially rotating, spherical shell); see Junk & Egbers (2000) for a review. The complexity of the global circulation pattern increases with  $Re$ . When  $Re$  is large enough, the flow becomes nonaxisymmetric and ultimately chaotic, e.g., Nakabayashi et al. (2002).

Figure 1 compares spherical Couette flow of a two-component, Hall-Vinen-Bekarevich-Khalatnikov (HVBK) superfluid at low and high  $Re$ . Meridional streamlines of the normal (i.e., torque generating) component are plotted for  $Re = 3 \times 10^2$  and  $3 \times 10^4$  in Figures 1a and 1b respectively. The flow is computed by integrating the HVBK equations (Hills & Roberts 1977) numerically using a pseudospectral collocation method (Canuto et al. 1988) with spectral filtering to suppress high spatial frequencies, especially at high  $Re$  (Peralta et al. 2005; Peralta 2006). We adopt no-slip and no-penetration boundary conditions for the normal component (velocity  $\mathbf{v}_n$ ), perfect slip for the superfluid component (i.e., no pinning, for numerical stability; velocity  $\mathbf{v}_s$ ), and a Stokes flow (with  $\mathbf{v}_n = \mathbf{v}_s$ ) initially. The mutual friction force is of the isotropic, Gorter-Mellink form ( $\propto v_{ns}^2 \mathbf{v}_{ns}$ , with  $\mathbf{v}_{ns} = \mathbf{v}_n - \mathbf{v}_s$ ) (Gorter & Mellink 1949), because the meridional counterflow in Figures 1a and 1b excites

<sup>1</sup> School of Physics, University of Melbourne, Parkville, VIC 3010, Australia

<sup>2</sup> Departamento de Física, Escuela de Ciencias, Universidad de Oriente, Cumaná, Venezuela

Kelvin waves via the Donnelly-Glaberson instability, converting the rectilinear vortex array into a vortex tangle (Swanson et al. 1983; Tsubota et al. 2003; Peralta et al. 2006b). The superfluid component also feels a vortex tension force  $\propto \boldsymbol{\omega}_s \times (\nabla \times \hat{\boldsymbol{\omega}}_s)$ , with  $\boldsymbol{\omega}_s = \nabla \times \mathbf{v}_s$ .

The meridional circulation pattern in Figure 1b is more complicated than in Figure 1a; seven cells are visible for  $Re = 3 \times 10^4$ , compared to only one cell for  $Re = 3 \times 10^2$ . The azimuthally averaged differential torque  $dN_z/d(\cos\theta)$  (Peralta et al. 2006b) is a monotonic function of latitude for  $Re = 3 \times 10^2$  but peaks near the (moving) secondary vortices (at  $\theta \approx 30^\circ$ ) in Figure 1b for  $Re = 3 \times 10^4$ .

The torque is variable at high  $Re$ , exhibiting persistent oscillations under steady differential rotation, whose amplitude depends on  $Re$  (Peralta et al. 2005). Figure 1c displays the torque on the outer sphere (stellar crust) as a function of time. For  $t \geq 20 \Omega^{-1}$ , with  $\Omega = 2\pi/P$ , after initial transients die away, we see that the torque is asymptotically steady for  $Re = 3 \times 10^2$  (solid curve) and oscillatory for  $Re = 3 \times 10^4$  (dashed curve). The variable torque leads naturally to rotational irregularities. The variability time-scale ( $\sim \Omega^{-1}$ ) is too fast to account for pulsar timing noise directly. However, the torque oscillates quasiperiodically, not periodically, so  $\Omega$  wanders stochastically when integrated over long times [c.f. micro-jumps and oscillations superimposed on a random walk; Boynton et al. (1972); Hobbs (2002)].

Of course, we wish to investigate the flow at  $Re \gtrsim 10^9$ , the realistic  $Re$  regime for radio pulsars (Mastrano & Melatos 2005). Unfortunately, our simulations cannot handle this. Even for  $Re = 10^5$ , and with heavy spectral filtering, the flow is unresolved numerically; the spectral coefficients do not decline monotonically with polynomial order as they should (Peralta 2006). From laboratory experiments, however, it is clear what to expect qualitatively as  $Re$  increases: the flow passes through a sequence of bifurcations to nonaxisymmetric states like herringbone waves and Stuart vortices at  $Re \sim 10^6$  (Junk & Egbers 2000), before developing fully into scale-free, Kolmogorov-like turbulence at  $Re \gtrsim 10^7$ , which itself is not always isotropic at small scales (Douady et al. 1991). Turbulent flow in He II at  $Re \gtrsim 10^5$  often contains a vortex tangle (Barenghi et al. 1997). Moreover, in experiments with He II, eddies in the normal and superfluid components match at scales larger than the average vortex separation (Barenghi et al. 1997), implying that, macroscopically, high- $Re$  superfluid turbulence behaves similarly to high- $Re$  classical turbulence. Hence, in neutron stars ( $Re \gtrsim 10^9$ ), the vortex tangle in the outer core may match its vorticity to the normal component. The vortex tension modifies this picture somewhat by contributing “stiffness” in regions where  $\boldsymbol{\omega}_s$  builds up (e.g., at the smallest scales in the Kolmogorov cascade). The largest eddies in fully developed turbulence, where the kinetic energy mainly resides, are nonaxisymmetric and move “jerkily”, so the net torque fluctuates substantially.

### 3. $Re$ DISTRIBUTION OF GLITCHING PULSARS

Given that the Reynolds number is a key factor governing the variability of the global superfluid flow in a neutron star, and hence the star’s rotation, it is interesting to test whether the amplitude and rate of incidence of rotational

irregularities depends on it. From the definition

$$Re = R^2 \Omega / \nu_n, \quad (1)$$

where  $R$  is the stellar radius and  $\nu_n$  is the kinematic viscosity of the normal component, it is clear that  $Re$  can be measured in principle, if we know how  $\nu_n$  depends on the density  $\rho$  and temperature  $T$  in the outer core. Using the Newtonian viscosity formula derived by Cutler & Lindblom (1987), due to neutron-neutron scattering, we find

$$Re = 1.8 \times 10^{11} (T/10^8 \text{ K})^2 (\Omega/10^2 \text{ rad s}^{-1}), \quad (2)$$

with  $\rho = 2.8 \times 10^{12} \text{ g cm}^{-3}$  (normal component) and  $R = 10^6 \text{ cm}$ . For electron-electron scattering in a superfluid, the multiplicative factor is  $6.0 \times 10^{10}$  (Andersson et al. 2005). In writing equations (1) and (2), we imagine a model where the outer core extends over the density range  $(2\text{--}4) \times 10^{14} \text{ g cm}^{-3}$ , where the superfluid behaves hydrodynamically (i.e., weak bulk pinning) and isotropically ( $^1\text{S}_0$ -paired). We assume that the normal component constitutes 1 % of the total density, to account for condensate depletion by nonideal effects. We do not treat stratification in the simulations to keep them tractable, although stratification is known to be important in suppressing meridional circulation (Abney & Epstein 1996; Peralta et al. 2006b).

The core temperature  $T$  is related to the surface temperature  $T_s$ , e.g., via the two-zone, heat-blanket model of Gudmundsson et al. (1982), which gives  $(T/10^8 \text{ K}) = 1.29(T_s/10^6 \text{ K})^{1.8}$ . Surface temperatures have been measured for 11 neutron stars, by fitting their thermal X-ray emission to hydrogen or heavy-element atmospheres (Larson & Link 2002; Page et al. 2004). However, the sample is too small to analyse statistically; only three of these objects exhibit glitches, for example. Instead, we are forced to estimate  $T_s$  from the characteristic age  $\tau_c = P/(2\dot{P})$ , combined with theoretical cooling curves, calibrated against the 11 objects above (Page 1998). We consider three cooling mechanisms: (I) standard neutrino cooling, via the Urca and modified Urca processes (Hoffberg et al. 1970), (II) nonstandard (fast) cooling due to paired neutron superfluidity (Amundsen & Østgaard 1985), and (III) nonstandard cooling with the superfluid energy gap fitted empirically to observations of thermal emission (Gnedin et al. 1994; Levenfish & Yakovlev 1996).

Figure 2a displays the raw  $Re$  distributions of the 67 glitching pulsars with  $\tau_c \leq 10^6 \text{ yr}$  (green histogram) and all 348 known pulsars with  $\tau_c \leq 10^6 \text{ yr}$  (red histogram), including the 67 glitchers. The objects are sorted into ten bins of equal logarithmic width 0.37 dex in the interval  $9.4 \leq \log_{10}(Re) \leq 13.1$ . Standard cooling (I) and Newtonian viscosity formulas are applied to both samples. We restrict attention to objects with  $\tau_c \leq 10^6 \text{ yr}$ , because the cooling curves compiled by Page (1998) drop away precipitously above this age, as neutrino cooling gives way to photon cooling (which depends sensitively on the uncertain composition of the stellar atmosphere).

The histogram in Figure 2a is redrawn for nonstandard cooling (II and III) in Figures 2b and 2c, with bin widths of 0.30 dex and 0.96 dex, respectively. Identical (after rescaling  $Re$ ) distributions are obtained if the superfluid electron-electron scattering viscosity is used instead.

The  $Re$  distribution of the glitching pulsars differs clearly from that of the total population. One sees im-

mediately, from Figure 2a, that most of the glitching pulsars have  $10^{11} \lesssim Re \lesssim 10^{12}$ , whereas the pulsar population peaks at  $10^{10} \lesssim Re \lesssim 10^{11}$ . To quantify this, we perform a Kolmogorov-Smirnov (K-S) test on the cumulative distributions constructed from Figure 2a (to circumvent binning bias). The K-S statistic is  $D = 0.3$ , yielding a probability  $p = 1 - 1.6 \times 10^{-5}$  that the two populations are drawn from different distributions. Similar conclusions follow for nonstandard cooling of types II and III, and for superfluid electron-electron scattering viscosity ( $p$  does not change when  $Re$  is rescaled multiplicatively). The associated K-S-probabilities are quoted in Table 1.

Is Figure 2 just a restatement of the well known trend that glitching pulsars tend to be young? Partly, but not entirely. The period distribution of glitching pulsars differs clearly from that of the total population, with a K-S probability  $p = 0.994$ . The maximum separation between the cumulative  $P$  distributions occurs at an intermediate period  $P = 0.32$  s, ruling out a pure age effect. [Observational studies of kick velocities and pulsars in supernova remnants suggest that the distribution of the birth periods is quite flat in the range  $0.05 - 0.5$  s; see Faucher-Giguère & Kaspi (2006), Ng & Romani (2007), and references therein.] It appears that  $P$  and  $\tau_c$  control glitch behaviour independently (perhaps, but not necessarily, through  $Re$ ). Interestingly, glitching pulsars are distributed differently in  $\tau_c$  and  $Re$ , peaking at  $\tau_c \sim 10^6$  yr (oldest objects) and  $Re \sim 10^{11}$  (intermediate objects) respectively.

Given that  $Re$  distributions of glitching and nonglitching pulsars are different, it is natural to ask whether the rate and amplitude of glitch activity are simple functions of  $Re$ . There are several possible measures of glitch activity in an individual pulsar. We pick three: (i) the activity parameter  $A_g = (N_g \Delta\Omega_g)/(t_g \Omega)$ , where  $N_g$  is the number of glitches observed over a total observation time  $t_g$  (taken to be the time since discovery, in the absence of complete data), and  $\Delta\Omega_g$  is the accumulated change in  $\Omega$  due to glitches (McKenna & Lyne 1990); (ii)  $\Delta\Omega_g/\Omega$ ; and (iii) the *mean* recurrence time  $t_r$  between glitches, normalized by  $\tau_c$  (in 11 out of 67 objects, this is an upper limit, as they have glitched once only). Interestingly, none of these measures show a clear trend with  $Re$ , leading to scatter plots. This suggests that  $Re$  controls the threshold for glitch activity, rather than its rate and amplitude, which is qualitatively consistent with §2. For example, one can imagine a  $Re$  threshold (when turbulence sets in), which must be exceeded for glitches to occur at all, and a separate “rate” threshold (perhaps controlled by the Rossby number, proportional to the crust-core shear), which determines how often the pulsar glitches per unit observation time (and hence  $A_g$ ). Likewise,  $t_r/\tau_c$  and  $\Delta\Omega_g/\Omega$  are related physically to the rate at which crust-core shear builds up, which is independent of  $Re$ . Also,  $A_g$  is not dimensionless, so it is not surprising that factors other than  $Re$  affect it. Note that  $Re$  decreases with  $\tau_c$  but varies independently with  $\Omega$ , so the  $A_g$ - $\tau_c$  correlation (Wang et al. 2000) is washed out in an  $A_g$ - $Re$  plot.

#### 4. DISCUSSION

A superfluid (or, indeed, a Newtonian fluid) contained in a differentially rotating, spherical shell circulates merid-

ionally and exerts a time-dependent viscous torque on the outer shell. The vigour of the circulation, and the variability of the torque, increase with  $Re$ ; the flow is steady for  $Re \lesssim 10^2$  and chaotic for  $Re \gtrsim 10^5$ . Spherical Couette flow is an idealised model of the superfluid outer core of a neutron star, in which the outer sphere is the stellar crust, which spins down electromagnetically. It is therefore interesting to test whether the incidence of pulsar rotational irregularities like glitches depends on  $Re$ . We show in §3 that this is indeed the case: the distribution of glitching and nonglitching pulsars with  $\tau_c \leq 10^6$  yr is different, with K-S probability  $\geq 1 - 3.9 \times 10^{-3}$ . This new fact joins the  $A_g$ -versus- $\tau_c$  correlation as one of the few observed regularities in glitch phenomenology.

An immediate worry is that the distributions in Figure 2 are contaminated by some observational selection effect. Our estimates of  $Re$  are uncertain in two ways. First,  $\tau_c$  is the characteristic spin-down age of the pulsar, not its true age. For example, five young pulsars with  $\tau_c \leq 1.7 \times 10^3$  yr have braking index  $n < 3$ , whereas the formula  $\tau_c = P/(2\dot{P})$  assumes  $n = 3$  (Melatos 1997; Livingstone et al. 2006). Second, the theoretical cooling curves depend sensitively on the superfluid energy gap in the outer core, which is poorly known (although admittedly calibrated by 11 pulsars with observed thermal emission). However, the above uncertainties do *not* affect the conclusion that the  $Re$  distributions of the glitching and nonglitching populations in Figure 2 are different, because  $T$  and hence  $Re$  are calculated in the same way for both samples. Indeed, it is hard to imagine that our ability to detect glitches in radio timing data is a function of  $Re$ .

Physically, the conclusions from Figure 2 are at once natural yet surprising. It is well known that torque variability increases with  $Re$  in a differentially rotating superfluid in laboratory and numerical experiments (§2). However, it is strange that pulsars behave differently at  $Re \lesssim 10^{10}$  (few glitches) and  $Re \gtrsim 10^{11}$  (many glitches). Naively, Kolmogorov turbulence should be scale-free, fully developed, and *indistinguishable* at these Reynolds numbers. There are at least two ways to explain this. First, processes involving microscopic superfluid turbulence, e.g., pinning (Alpar et al. 1984) and vortex tangle formation (Peralta et al. 2006b), may depend sensitively on  $Re$  in the range  $10^{10} \leq Re \leq 10^{11}$ . Second, it is possible that theoretical estimates of  $Re$  (Andersson et al. 2005; Mastrano & Melatos 2005) are  $\sim 10^6$  times too high. If so, this reduces the peak of the glitching pulsar distribution to  $Re \lesssim 10^5$ , exactly where spherical Couette flow breaks up into nonaxisymmetric modes before becoming chaotic (§2). We have no reason to doubt the  $\nu_n$  carefully derived in the literature. However, if the flow is turbulent, Reynolds stresses may completely overwhelm viscous stresses, such that  $\nu_n$  is replaced by  $\nu_n + A$ , where  $A$  satisfies  $A \partial v_i / \partial x_j \approx \langle \delta v_i \delta v_j \rangle$ ,  $v_i$  is the mean velocity, and  $\delta v_i$  is the fluctuating velocity (zero average) (Pedlosky 1982). Typically, we have  $A/\nu_n \sim (\delta v/v)^2 Re \gg 1$ . Turbulent Reynolds stresses drastically reduce  $Re$  in a range of geophysical and astrophysical applications (Pedlosky 1982).

Plainly, there exist several high- $Re$  pulsars that do not glitch. Observational selection effects aside, there exist several theoretical mechanisms that may be responsible. First, for spherical Couette flow in the range  $10^3 < Re <$

$10^7$ , there are sizable intervals of  $Re$  where the flow is almost laminar, interposed between intervals where it is turbulent (Nakabayashi & Tsuchida 2005). Second, for  $Re > 10^7$ , where the turbulence is fully developed (Kolmogorov) and “isotropic” when averaged over a turn-over time, the torque on the star is steadier than for organised modes (e.g., Taylor-Görtler vortices) near the onset of turbulence ( $Re \sim 10^5$ ), which are not isotropic on average. Third, if atmospheres and planetary interiors are any guide, the turbulent Reynolds stresses depend sensitively on what nonlinear modes are excited in the turbulence, and the effective  $Re$  may vary greatly (and unpredictably) from object to object, in ways not captured by (2). Incidentally, none of the pulsars in our sample have low  $Re$ , even after adjusting for turbulent Reynolds stresses; the minimum is  $Re \sim 10^3$ . Hence there are no examples of low- $Re$  objects that glitch unexpectedly.

In closing, we emphasize that the results of this paper do *not* prove that superfluid turbulence exists in a neutron star, let alone that it controls glitch behaviour. However, considerable effort has been expended to identify patterns

in glitch behaviour, with limited success. The undeniable empirical fact that the  $Re$  distributions in Figure 2 are different is therefore intriguing, especially because  $Re$  is a *dimensionless* quantity with *deep hydrodynamical significance*, and because the K-S comparison is robust with respect to how  $T$ ,  $\nu_n$ , and hence  $Re$  are estimated observationally. One hopes it will offer an enlightening clue to glitch physics, whether or not superfluid turbulence turns out to play a central role. We also hope that the results presented here will stimulate the ongoing observational campaign to measure pulsar temperatures.

This research was supported by a postgraduate scholarship from the University of Melbourne and the Albert Shimmings writing-up award. It makes use of the ATNF pulsar catalogue <http://www.atnf.csiro.au/research/pulsar/psrcat> (Manchester et al. 2005) and unpublished glitch data provided kindly by D. Lewis, M. Kramer, and A. Lyne (private communications, 2005). We thank the anonymous referee for helpful suggestions.

## REFERENCES

- Abney, M., & Epstein, R. I. 1996, *J. Fluid Mech.*, 312, 327  
 Alpar, M. A., Pines, D., Anderson, P. W., & Shaham, J. 1984, *ApJ*, 276, 325  
 Amundsen, L., & Østgaard, E. 1985, *Nucl. Phys. A*, 437, 487  
 Andersson, N., Comer, G. L., & Glampedakis, K. 2005, *Nucl. Phys. A*, 763, 212  
 Barenghi, C. F., Samuels, D. C., Bauer, G. H., & Donnelly, R. J. 1997, *Phys. Fluids*, 9, 2631  
 Boynton, P. E., Groth, E. J., Hutchinson, D. P., Nanos, G. P., Partridge, R. B., & Wilkinson, D. T. 1972, *ApJ*, 175, 217  
 Canuto, C., Hussaini, M., Quarteroni, A., & Zang, T. 1988, *Spectral Methods in Fluid Dynamics* (Springer-Verlag)  
 Cutler, C., & Lindblom, L. 1987, *ApJ*, 314, 234  
 Douady, S., Couder, Y., & Brachet, M. E. 1991, *Phys. Rev. Lett.*, 67, 983  
 Faucher-Giguère, C.-A., & Kaspi, V. M. 2006, *ApJ*, 643, 332  
 Gnedin, O. Y., Yakovlev, D. G., & Shibano, Y. A. 1994, *Astron. Lett.*, 20, 409  
 Gorter, C. J., & Mellink, J. H. 1949, *Physica*, 85, 285  
 Greenstein, G. 1970, *Nature*, 227, 791  
 Gudmundsson, E. H., Pethick, C. J., & Epstein, R. I. 1982, *ApJ*, 259, L19  
 Hills, R. N., & Roberts, P. H. 1977, *Arch. Rat. Mech. Anal.*, 66, 43  
 Hobbs, G. 2002, PhD thesis, University of Manchester  
 Hobbs, G., Manchester, R., Teoh, A., & Hobbs, M. 2004, in *IAU Symposium*, 139+  
 Hoffberg, M., Glassgold, A. E., Richardson, R. W., & Ruderman, M. 1970, *Phys. Rev. Lett.*, 24, 775  
 Hollerbach, R. 1998, *Phys. Rev. Lett.*, 81, 3132  
 Janssen, G. H., & Stappers, B. W. 2006, *astro-ph/0607260*  
 Junk, M., & Egbers, C. 2000, *LNP Vol. 549: Physics of Rotating Fluids*, 549, 215  
 Krawczyk, A., Lyne, A. G., Gil, J. A., & Joshi, B. C. 2003, *MNRAS*, 340, 1087  
 Larson, M., & Link, B. 2002, *MNRAS*, 333, 613  
 Levenfish, K. P., & Yakovlev, D. G. 1996, *Astron. Lett.*, 22, 49  
 Li, Y. 2004, *Sci. China Ser. A*, 47, 81  
 Livingstone, M. A., Kaspi, V. M., Gotthelf, E. V., & Kuiper, L. 2006, *ApJ*, 647, 1286  
 Manchester, R. N., Hobbs, G. B., Teoh, A., & Hobbs, M. 2005, *Astron. J.*, 129, 1993  
 Marcus, P., & Tuckerman, L. 1987, *J. Fluid Mech.*, 185, 31  
 Mastrano, A., & Melatos, A. 2005, *MNRAS*, 361, 927  
 McKenna, J., & Lyne, A. G. 1990, *Nature*, 343, 349  
 Melatos, A. 1997, *MNRAS*, 288, 1049  
 Middleditch, J., Marshall, F. E., Wang, Q. D., Gotthelf, E. V., & Zhang, W. 2006, *astro-ph/0605007*  
 Nakabayashi, K., Sha, W., & Tsuchida, Y. 2005, *J. Fluid Mech.*, 534, 327  
 Nakabayashi, K., & Tsuchida, Y. 2005, *Phys. Fluids*, 17, 4110  
 Nakabayashi, K., Tsuchida, Y., & Zheng, Z. 2002, *Phys. Fluids*, 14, 3963  
 Ng, C. ., & Romani, R. W. 2007, *ArXiv Astrophysics e-prints*  
 Page, D. 1998, in *Neutron Stars and Pulsars: Thirty Years after the Discovery*, 183+  
 Page, D., Lattimer, J. M., Prakash, M., & Steiner, A. W. 2004, *ApJS*, 155, 623  
 Pedlosky, J. 1982, *Geophysical fluid dynamics* (New York and Berlin, Springer-Verlag, 1982. 636 p.)  
 Peralta, C. 2006, PhD thesis, University of Melbourne  
 Peralta, C., Melatos, A., Giacobello, M., & Ooi, A. 2005, *ApJ*, 635, 1224  
 —. 2006a, *ApJ*, 644, L53  
 —. 2006b, *ApJ*, 651, 1079  
 Shemar, S. L., & Lyne, A. G. 1996, *MNRAS*, 282, 677  
 Swanson, C. E., Barenghi, C. F., & Donnelly, R. J. 1983, *Phys. Rev. Lett.*, 50, 190  
 Tsakadze, J. S., & Tsakadze, S. J. 1980, *J. Low Temp. Phys.*, 39, 649  
 Tsubota, M., Araki, T., & Barenghi, C. F. 2003, *Phys. Rev. Lett.*, 90, 205301  
 Urama, J. O., & Okeke, P. N. 1999, *MNRAS*, 310, 313  
 Wang, N., Manchester, R. N., Pace, R. T., Bailes, M., Kaspi, V. M., Stappers, B. W., & Lyne, A. G. 2000, *MNRAS*, 317, 843

Cooling	$p$
I	$1 - 6.4 \times 10^{-5}$
II	$1 - 3.9 \times 10^{-3}$
III	$1 - 2.5 \times 10^{-3}$

TABLE 1  
K-S PROBABILITIES  $p$  FOR NEWTONIAN VISCOSITY AND THREE COOLING MECHANISMS.

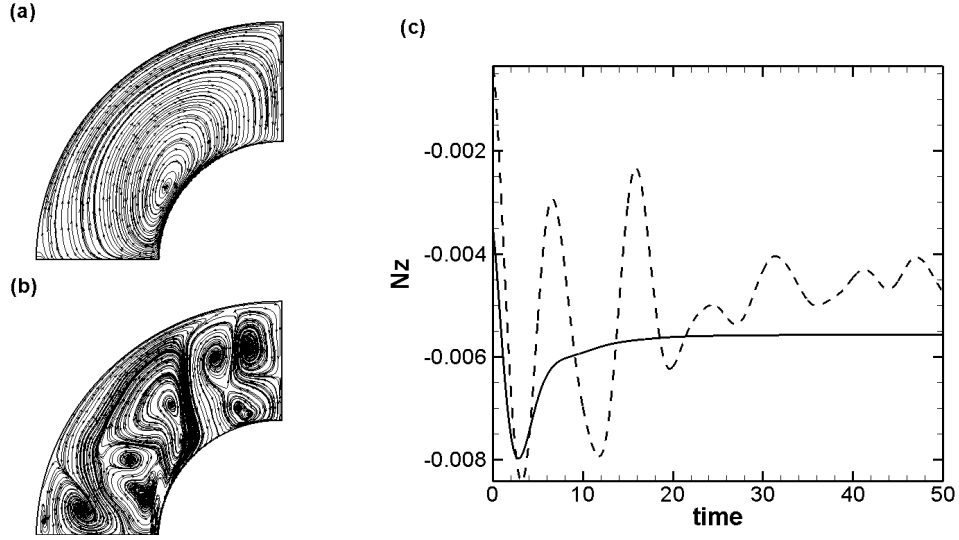


FIG. 1.— Snapshot at  $t = 50\Omega^{-1}$  of meridional streamlines (computed by integrating the in-plane velocity vector) for the normal fluid component in spherical Couette flow in the outer core of a neutron star for (a)  $Re = 3 \times 10^2$  and (b)  $Re = 3 \times 10^4$ . (c) Evolution of the outer torque on the crust (in units of  $\rho R^5 \Omega^2$ ) for  $Re = 3 \times 10^2$  (solid curve) and  $Re = 3 \times 10^4$  (dashed curve). The simulation parameters are mutually ordered as in the outer core of a neutron star but exaggerated for computational tractability, viz., crust-core angular velocity shear  $\Delta\Omega/\Omega = 0.3$ , dimensionless shell thickness  $\delta = 0.5$ , stiffness parameter  $\nu_s = 10^{-5} R^2 \Omega \ll \nu_n$ , Gorter-Mellink constant  $A' = 5.8 \times 10^{-2}$ , and superfluid density fraction  $\rho_s/\rho = 0.99$ . We follow exactly the notation and definitions in Peralta et al. (2005).

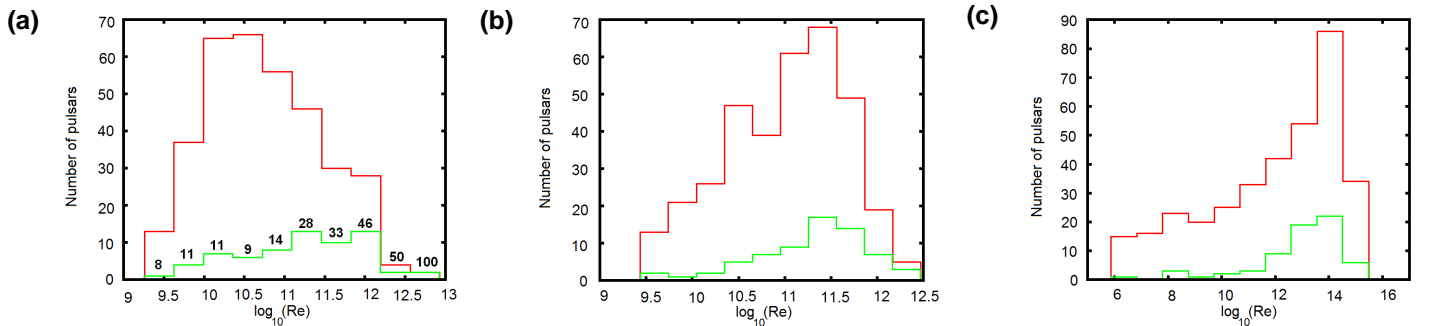


FIG. 2.— Reynolds number distribution for the 67 glitchers (green curve) and all 348 pulsars (red curve, including the 67 glitchers) with characteristic age  $\tau_c \leq 10^6$  yr, using (a) standard neutrino cooling, (b) nonstandard (fast) cooling due to paired neutron superfluidity, and (c) nonstandard cooling with the superfluid energy gap fitted empirically to observations of thermal emission. The data are divided into 10 bins of equal logarithmic width (a) 0.37, (b) 0.30, and (c) 0.96. The percentage of objects that glitch in each bin, for standard neutrino cooling, is recorded above the histogram in (a).